Mechanism, Kinetics and Potential Morphological Consequences of Solid-State Polymerization

Rangarajan Srinivasan,‡ Celine Almonacil,† Sujatha Narayan,‡ Prashant Desai,‡ and A. S. Abhiraman*,†

Schools of Chemical Engineering and Textile and Fiber Engineering, Polymer Education and Research Center, Georgia Institute of Technology, Atlanta, Georgia 30332

Received April 30, 1998; Revised Manuscript Received July 27, 1998

ABSTRACT: The likely mechanism which allows the required migration of functional groups for solid-state polymerization (SSP) of polyamides and polyesters is shown to be interchange reactions. This "chemical diffusion" of functionality has exactly the same mathematical form as that of classical diffusion of small molecules. The consequent model for kinetics of SSP in fine geometries is seen to fit experimental data well. It yields an estimate of the critical distance over which the functionality jumps with each interchange reaction. The critical reaction distance thus obtained, ~5 Å, is similar to those determined from diffusion-controlled reactions of small molecules. The profound changes that interchange reactions can produce during SSP in the topology of chain segments in the intercrystalline regions of flexible and semirigid polymers, especially in oriented structures, are revealed.

Introduction

It is well-known that many properties of polymeric materials can be improved with increase in molecular weight. With step-growth polymers such as polyamides and polyesters, one of the routes to high molecular weight has been through solid-state polymerization (SSP). This is achieved by heating these polymers in an inert atmosphere to a temperature well above their glass transition, but below melting. Solid-state polymerization can produce a substantial increase in the degree of polymerization of the polymer, while the material still retains its solid shape.

Preextrusion SSP of condensation polymers, where it is carried out in the form of chips or powders, has become a common feature in the production of polymers for industrial fibers or molded products. Several recent literature reviews relate the history of SSP.[1,2] If carried out after the initial shaping operation, e.g. in fibers or thin films, it is termed as postextrusion SSP. This process, still at the developmental stage, potentially offers several advantages over traditional preextrusion SSP. There is a limit to the molecular weight that can be achieved through preextrusion SSP, mainly because of diffusion limitations in relatively large particles. The probability that the condensation product of polymerization can react to cause depolymerization before it can be removed from the particle is high in this case. In addition, processing problems such as high pressures, thermomechanical degradation, melt fracture, and filament breakage, can occur during subsequent extrusion of the high molecular weight polymer. With postextrusion SSP of stoichiometrically balanced compositions, no limit has yet been observed to the molecular weight that can be obtained, especially if carried out in the form of fibers and thin films. Since these geometries have at least one dimension that is much smaller compared to chips, the condensation product can be more effectively removed before it can react in the system.

* To whom correspondence should be addressed.
† School of Chemical Engineering
‡ School of Textile and Fiber Engineering

While the kinetics of solid-state polymerization in polymer chips has been studied in detail, the kinetics in finer geometries has not been explored adequately. The kinetics in the latter case might not be controlled by the diffusion of byproducts of the reaction but by the diffusion of reactive end groups in the system. For example, Srinivasan et al. found that SSP of nylon 66 fibers at and above 220 °C follows step-growth bulk polymerization kinetics.[3] Chen et al. found that the SSP of nylon 66 flakes was reaction-controlled.[4] Gaymans et al. also found that the rate of SSP of fine powders of nylon 6 was limited by the diffusion of the reacting (acid) chain end group.[5] Mallon and Ray have recently modeled the reactions and mass-transfer aspects of solid-state polycondensation, and the consequent issues in reactor design.[6,7] In the crystallized solid state, the relatively rapid buildup of molecular weight cannot be rationalized by diffusion of the molecules or their segments, a mechanism which permits frequent encounters of reacting groups in the melt state. Migration of end groups over relatively large distances would be required to yield a significant increase in molecular weight. Thermal motions are severely restricted in the solid state, and segmental diffusion is considerably restricted as compared to the melt state.[1,8,9] In addition, in well-crystallized semicrystalline polymers, the motion of chain segments is restrained by the fact that almost all of them are anchored in crystals.

Interchange reactions can play a fundamental role in this regard by providing a mechanism for end group functionality to migrate and thus facilitate polymerization. Interchange reactions in the melt state, such as the acid−amide and amine−amide interchanges in polyamides, or the alcohol−ester and acid−ester interchanges in polyesters, have been extensively studied.[1,10] However, interchange reactions in the solid state have not received much attention.[1]

There have been a few direct attempts to explore solid-state interchange reactions in poly(ethylene terephthalate), using ^{1}H NMR or small-angle neutron scattering.[11−13] However, these studies, done at lower temperatures and shorter times than typical solid-state

S0024-9297(98)00693-7 CCC: $15.00
Published on Web 09/10/1998

Table 1. Specifications of the Starting Materials, As-Extruded Fibers of Nylon 66 and Nylon 46

parameter	nylon 66	nylon 46
molecular weight M_v (g/mol)	40 000	41 000
spinning speed (m/min)	300	500
linear density (dtex)	7000	1050
no of filaments	210	36
tenacity (cN/dtex)	1.01	1.50
elongation to break (%)	412	450
melting point (°C) (DSC onset)	248	280

polymerization, did not produce any conclusions with regard to whether interchange reactions occurred to a significant extent during solid state polymerization, and did not provide insight with regard to the dominant reaction in systems which can undergo two or more reactions. There is extensive indirect evidence of interchange reactions during SSP. In a series of papers, Lenz et al. studied reorganizations in various copolymers, mainly copolyesters. They found an increase in the extent of blockiness which *requires* the occurrence of a significant extent of interchange reactions.[13,14] Upon heat treatment in the solid state, a partially crystalline copolymer can develop an increasingly blocky structure if its repeating units can undergo interchange reactions in such a way that the newly interchanged units can be taken into the crystalline regions and thus become inaccessible to further reaction. The process is thus a reaction-facilitated crystallization. The results also show that the interchange reactions are essentially restricted to the noncrystalline regions.

Fitzgerald et al. explicitly recognized interchange reactions to be responsible for migration of functionality in solid-state polymerization of poly(*p*-phenylene terephthalamide) in the region around 500 °C.[15] They concluded that catalysts simply facilitated amine–amide interchange and found that interchange reactions could occur in the solid state even without catalysts.

A review of the literature shows clearly that the occurrence of interchange reactions during SSP has been recognized by many researchers. However, with the exception of Fitzgerald et al.,[15] who inferred it to be the mechanism for SSP in poly(*p*-phenylene terephthalamide), it has not been recognized as the necessary or dominant mechanism in SSP of semirigid or flexible polymers. Also, with the exception of the work by Lenz et al.[13,14] on evolution of crystallizable block sequences, the morphological consequences of SSP, especially in oriented structures, have not been reported.

The research reported here emphasizes fundamental aspects of the mechanism that governs solid-state polymerization in polyamides and polyesters, the consequent kinetics and its morphological implications. We show here that interchange reactions provide the dominant mechanism for the required migration of functionality to facilitate chain extension. Data from solid-state polymerization in filaments of nylon 66 and nylon 46 are used to provide quantitative justification for the proposed mechanism and the kinetic model based on it.

Experimental Details

Materials. The step-growth polyamides chosen for this research were nylon 66 and nylon 46. Partially crystalline filaments of nylon 66 and nylon 46, obtained by melt extrusion at low speeds, were used. The material specifications of the two fibers are given in Table 1. The data for kinetics of solid-state polymerization of nylon 66 were reported previously.[3]

Solid-State Polymerization. Skeins of fibers were placed unconstrained in a tubular oven and heated to 105 °C in nitrogen (high purity grade) for 1 h to dry the samples. The temperature of the oven was then raised to the polymerization temperature at a rate of 20 °C/min and then maintained for the required period of time. The variation at maximum temperature was less than ±2 °C. The samples were then allowed to cool in a stream of nitrogen to room temperature. The nitrogen flow rate was maintained constant at 30 ft^3/h (0.8 m^3/h) throughout the experiment. This procedure is similar to the one reported by us previously.[3]

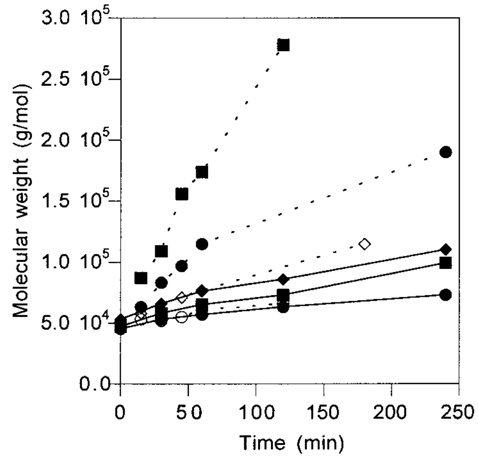

Figure 1. Viscosity average molecular weight as a function of time of SSP of nylon 66 and nylon 46. The lines are drawn for visualization purposes. The solid line corresponds to nylon 46; the dashed lines, to nylon 66: (○) T = 220 °C, (◇) T = 230 °C, (●) T = 240 °C, (■) T = 250 °C, (◆) T = 260 °C.

Dilute Solution Viscometry. The flow times of solutions of concentrations 0.1, 0.2, and 0.4 g/dL in 90% formic acid at 25 °C were measured and the intrinsic viscosity, [η], was calculated from these measurements. The viscosity average molar mass ($\bar{M}_v$) was then calculated using the Mark–Houwink equation

$$[\eta] = K(\bar{M}_v)^a \tag{1}$$

The Mark–Houwink parameters, K and a, used for nylon 66/formic acid at 25 °C are 0.0353 cm^3/g and 0.786, respectively. The Mark–Houwink parameters used for nylon 46/formic acid at 25 °C are 0.0464 cm^3/g and 0.76, respectively.[16]

Results and Discussion

Kinetics of Solid-State Polymerization of Polyamides. As previously reported,[3] molecular weights up to 280 000 g/mol have been obtained in nylon 66 from a starting molecular weight of 40 000 g/mol, which corresponds to a 7-fold increase in molecular weight. As Figure 1 shows, temperature has a significant effect on the rate of polymerization for both polymers, and the extent and rate of increase in molecular weight are both significantly higher in nylon 66 as compared to nylon 46. With nylon 46, molecular weights only up to 110 000 g/mol can be achieved in solid-state polymerization after 4 h, corresponding only to a 3-fold increase. It should be noted that the zero time here corresponds to the time at the peak solid-state polymerization temperature and the corresponding molecular weight is therefore slightly higher than that of the as-extruded fibers.

Molecular weight versus time data for nylon 66 were fitted to first-, second-, and third-order reaction kinetics, assuming stoichiometric amounts of carboxylic acid and amine end functional groups, as shown in Figure 2. These results show that solid-state polymerization of nylon 66 follows typical step-growth polymerization kinetics.

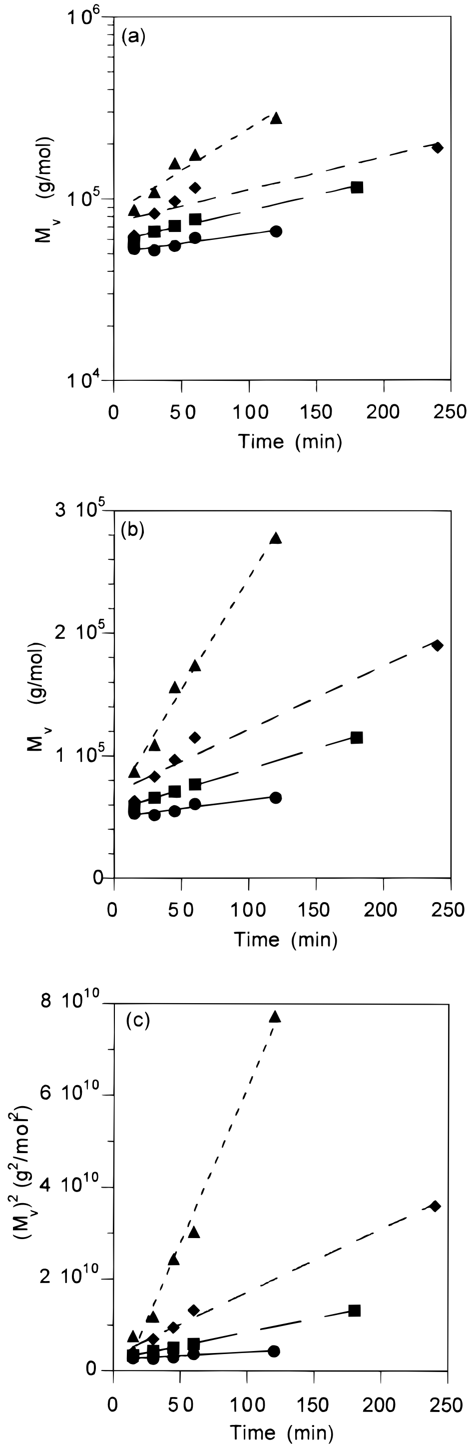

Figure 2. Kinetic fits of molecular weight data for SSP of nylon 66: (a) first order (b) second order (c) third order. Temperatures: (▲) 220 °C; (◆): 230 °C; (■) 240 °C; (●) 250 °C.

Equally good degrees of fit could be obtained with second- and third-order reaction kinetics. The fit to first-order kinetics is poor.

The rate constants for solid-state polymerization of nylon 66 were calculated assuming that (i) all the chain ends (functional groups for polymerization) existed in the noncrystalline phase and that (ii) the mass fraction crystallinity, X_c, of the polymer remained constant throughout the course of solid-state polymerization.

Since all the end groups are assumed to be in the noncrystalline phase, the concentration of end groups

Table 2. Second- and Third-Order Overall Rate Constants for SSP of Nylon 66 and Nylon 46, Obtained Assuming a Noncrystalline Density of 1 g/cm³

SSP temperature (°C)	nylon 66: second-order rate constant [(mol/g)$^{-1}$ s^{-1}]	nylon 66: third-order rate constant $\times 10^{-4}$ [(mol/g)$^{-2}$ s^{-1}]
220	0.8	1.7
230	1.9	6.1
240	3.0	14.2
250	10.6	68.2

has to be calculated with respect to the noncrystalline phase, i.e.,

$$[\mathrm{M}^*] = \frac{[\mathrm{M}]}{(1 - X_c)} \tag{2}$$

where [M*] is the concentration of each of the end groups in moles per gram of *noncrystalline phase* of polymer, and [M] is the concentration of the end groups in moles per gram of polymer. The reaction rate can then be described as

$$\frac{\mathrm{d}[\mathrm{M}^*]}{\mathrm{d}t} = k[\mathrm{M}^*]^n \tag{3}$$

where k is the reaction rate constant and n is the order of the reaction. Integration of eq 3 with initial concentration, $[\mathrm{M}^*]_o$, gives

$$\frac{(1 - X_c)^{n-1}}{([\mathrm{M}^*]_t)^{n-1}} - \frac{(1 - X_c)^{n-1}}{([\mathrm{M}^*]_o)^{n-1}} = (n - 1)kt \tag{4}$$

Since the number average molecular weight $M_n = 1/[\mathrm{M}]$ for a linear polymer with stoichiometric balance of end groups, eq 4 becomes

$$(M_n)^{n-1} - (M_{n0})^{n-1} = \frac{(n - 1)}{(1 - X_c)^{n-1}}kt \tag{5}$$

If we assume that the molecular weight distribution of the system remains the same as that of a typical step-growth polymerization reaction, with $M_w/M_n \approx 2$ and that the weight and viscosity average molecular weights are approximately the same ($M_w \approx M_v$), then the initial and final viscosity average molecular weights can be related as follows

$$(M_v)^{n-1} - (M_{v0})^{n-1} = \frac{(n - 1)2^{n-1}}{(1 - X_c)^{n-1}}kt \tag{6}$$

For a second-order reaction ($n = 2$), eq 6 reduces to

$$M_v - M_{v0} = \frac{2}{(1 - X_c)}kt \tag{7}$$

while, for a third-order reaction ($n = 3$), eq 6 reduces to

$$(M_v)^2 - (M_{v0})^2 = \frac{8}{(1 - X_c)^2}kt \tag{8}$$

The rate constants for the second- and third-order reaction kinetics at the four different temperatures, calculated from the data in Figure 2, are given in Table 2. The crystallinity was taken to be 30%. Wide-angle X-ray crystallinity data obtained by Ruland's method

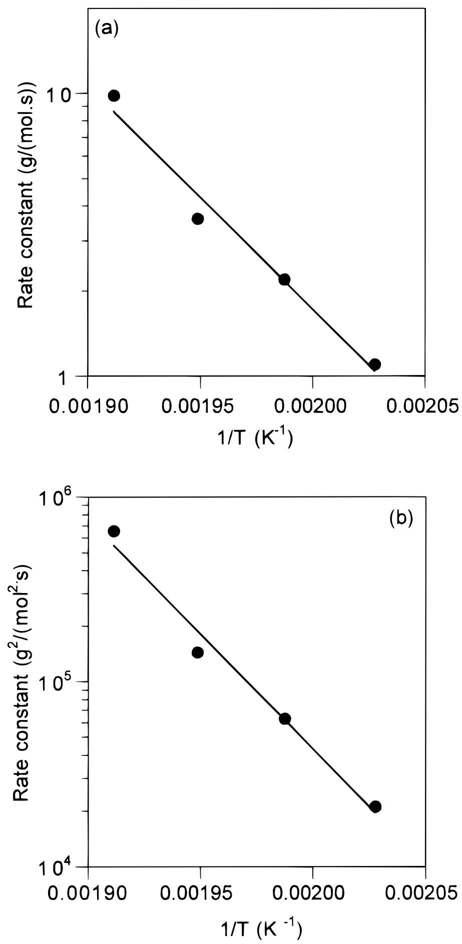

Figure 3. Arrhenius plots for overall polymerization rate constant: (a) second-order kinetics and (b) third-order kinetics.

showed that the crystallinity was approximately constant during solid-state polymerization. While the as-extruded fibers had a crystallinity of 25%, the crystallinity after solid-state polymerization ranged from 32 to 35%.[17] The Arrhenius plots of second- and third-order reactions are shown in Figure 3 from which the activation energies were calculated to be 42 and 61 kcal/mol for the second- and third-order reactions, respectively.

Roerdink and Warnier showed that the extent and rate of molecular weight build-up in nylon 46 are both inhibited by the irreversible pyrrolidine formation reaction:[18]

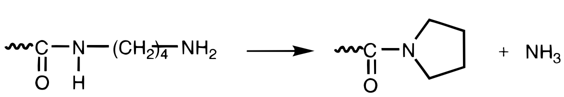

By reducing the number of amine end groups available for solid-state polymerization, the pyrrolidine formation is responsible for the inhibited rate and extent of increase in molecular weight of this polymer. In addition, the competing reactions produce a stoichiometric imbalance that complicates the kinetics of solid-state polymerization of nylon 46. Determination of two rate constants, one for polymerization and one for pyrrolidine formation, and complete knowledge of initial functional group concentration, are necessary to fully describe the kinetics of nylon 46. Therefore, analyzing the evolution of the molecular weight for nylon 46 is significantly more complicated than for nylon 66 and would require accurate determination of number average molecular weight and end group concentrations.

Migration of Functionality via Interchange Reaction: Kinetic Implications. As discussed earlier, the kinetics of solid-state polymerization in fine geometries, such as fibers and thin films, might not be controlled by the diffusion of byproducts of the reaction but by the diffusion of reactive end groups in the system. Interchange reactions offer a mechanism through which the end-group functionality can migrate and thus facilitate polymerization. If interchange reactions constitute the mechanism through which functional groups migrate randomly to the vicinity of each other for polymerization in the solid-state, the governing equations can be shown to be mathematically equivalent to those of diffusion-controlled bimolecular reactions of small molecules. The equivalence arises from the fact that each interchange reaction of an end group occurs within a critical distance and the functionality hops over this critical distance as a consequence. The frequency of reaction of an end functional group, together with this hop distance, determines an effective diffusion coefficient for a functional group. Thus solid-state polymerization becomes analogous to a diffusion-controlled bimolecular reaction with one or both species diffusing through the system, depending on whether one or both functional groups in a polymer undergoes exchange reactions. The following is a brief summary of kinetics of diffusion-controlled bimolecular reactions.[19]

Diffusion-Controlled Bimolecular Reactions. The rate at which the two molecules, A and B, get close to one another in a mixture is governed by the phenomenological laws of diffusion. If we consider the diffusion of a system of A and B molecules, with stationary B molecules, the concentration of A at the surface of B should be zero, while the concentration at a large distance from B is equal to the bulk concentration, C_{A0} ($C_A = C_{A0}$ when $r = \infty$ and $C_A = 0$ when $r = \delta$, where δ is the distance of closest approach for reaction). Assuming that all A molecules react once they are within a distance δ of the B molecules, the rate of reaction is equal to the total flux through the surface of a sphere of radius δ around B. If steady state is assumed and the diffusion process is taken to be spherically symmetric, i.e., isotropic, the total flux through the surface of a sphere of radius δ around B, I_A, is[19]

$$I_A = 4\pi r^2 D_A \frac{\mathrm{d}C_A}{\mathrm{d}r} \tag{9}$$

where D_A is the diffusion coefficient of A. Equation 9 can be integrated if the diffusion coefficient is independent of concentration. By integrating eq 9 from $r = \delta$ to $r = \infty$, the rate of reaction R_A is then found to be

$$R_A = 4\pi\delta D_A C_{A0} \tag{10}$$

If B molecules are not stationary but also undergo motion, it can be taken into account by replacing D_A by $(D_A + D_B)$.[19] Then eq 10 becomes

$$R_A = 4\pi\delta(D_A + D_B)C_{A0}C_{B0} \tag{11}$$

If the diffusion coefficient and the rate of the reaction are known, then δ, the critical reaction distance or the distance of closest approach for reaction, can be calculated. In the case of small molecules, this distance has been estimated to be around 5 Å.[19]

Kinetic Model of Solid-State Polymerization. A kinetic scheme which is mathematically equivalent to that of the above-described bimolecular reactions can be formulated for the case where interchange reactions cause migration and facilitate collision of end functional groups in solid-state polymerization. We consider here, as an example, solid-state polymerization of polyamides. The solid-state polymerization of polyesters will be presented later. The following assumptions have been made: (i) all the chain ends are in the noncrystalline phase; (ii) the mass fraction crystallinity of the polymer is constant throughout the course of the reaction; and (iii) the change in amide ([CONH]) group concentration during the course of polymerization is negligible.

For polyamides, the two interchange reactions which can produce migration of end group functionality are the amine−amide interchange, referred to with subscript 1, and the acid−amide interchange, referred to with subscript 2 (see Figure 4). The generalized reaction rates of the two interchange reactions can be written as

$$R_1 = k_1[\mathrm{M_1}^*]^m[\mathrm{A}^*]^n \tag{12}$$

$$R_2 = k_2[\mathrm{M_2}^*]^p[\mathrm{A}^*]^q \tag{13}$$

where the two end groups, NH_2 and COOH, are referred to as M_1* and M_2* respectively, k_1 and k_2 are the corresponding interchange rate constants and [A*] is the amide group concentration in the noncrystalline phase. The frequency of interchange reactions, ϕ_1 and ϕ_2, of an end group can be calculated as follows:[20]

$$\phi_1 = \frac{k_1[\mathrm{M_1}^*]^m[\mathrm{A}^*]^n}{[\mathrm{M_1}^*]} = k_1[\mathrm{M_1}^*]^{m-1}[\mathrm{A}^*]^n \tag{14}$$

$$\phi_2 = \frac{k_2[\mathrm{M_2}^*]^p[\mathrm{A}^*]^q}{[\mathrm{M_2}^*]} = k_2[\mathrm{M_2}^*]^{p-1}[\mathrm{A}^*]^q \tag{15}$$

If δ_1 and δ_2 represent the reaction distances for the interchange reactions 1 and 2, respectively, then the mean square distance moved by each end group per unit time is given by[20]

$$\langle r_1^2\rangle = \phi_1\delta_1^2 \tag{16}$$

$$\langle r_2^2\rangle = \phi_2\delta_2^2 \tag{17}$$

The diffusion coefficient of the end groups can then be calculated, using Einstein's relation, as[21]

$$D_1 = \frac{\langle r_1^2\rangle}{6} \tag{18}$$

$$D_2 = \frac{\langle r_2^2\rangle}{6} \tag{19}$$

If we assume that the critical distance for polymerization of the two end groups is δ, then the rate at which end groups encounter, R_e, is given by

$$R_e = 4\pi(D_1 + D_2)\delta[\mathrm{M_1}^*][\mathrm{M_2}^*]N_a^{\,2}\rho_A \tag{20}$$

where N_a is Avogadro's number and ρ_A is the density of the amorphous phase. The rate of encounters is then expressed in (number/per gram of noncrystalline phase)/second. Since we assume that the reaction proceeds instantaneously once the end groups are within the critical reaction distance of one another, the polymerization rate, R_p, can be directly obtained from the rate of encounters (eq 20). It is thus given by

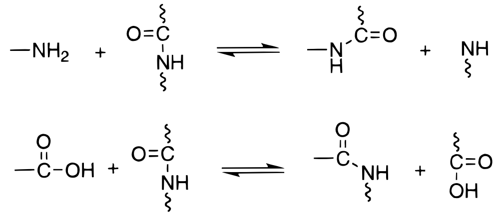

Figure 4. Amine−amide (top) and acid−amide (bottom) interchange reactions in polyamides.

$$R_p = R_e/N_a = 4\pi(D_1 + D_2)\delta[\mathrm{M_1}^*][\mathrm{M_2}^*]N_a\rho_A \tag{21}$$

where the polymerization rate is expressed in (moles per gram of noncrystalline phase)/second.

From eqs 14, 16, and 18, the effective diffusion coefficient for amine end group functionality is given by

$$D_1 = {}^1\!/_6\,\delta_1^{\,2}k_1[\mathrm{M_1}^*]^{m-1}[\mathrm{A}^*]^n \tag{22}$$

where k_1 is the rate constant for the amine−amide interchange reaction. Since the rate constant for amine−amide interchange is known to be much higher than that of acid−amide exchange,[22] the latter is neglected. Therefore, the effective diffusion coefficient for acid end group functionality, D_2, is taken to be zero.

From eqs 20 and 22, the effective rate of solid-state polymerization of polyamides is then found to be

$$R_p = {}^2\!/_3\,\pi\delta_1^{\,2}\delta k_1[\mathrm{A}^*]^n[\mathrm{M_1}^*]^m[\mathrm{M_2}^*]N_a\rho_A \tag{23}$$

For simplicity, we assume all the critical reaction distances to be the same ($\delta_1 = \delta$), giving

$$R_p = {}^2\!/_3\,\pi\delta^3 k_1[\mathrm{A}^*]^n[\mathrm{M_1}^*]^m[\mathrm{M_2}^*]N_a\rho_A \tag{24}$$

It has been reported that the amine−amide interchange reaction is of first order in amine and amide group concentration (i.e., $m = n = 1$).[22] Also, the change in amide link concentration during the course of solid-state polymerization is negligible. Then the overall rate of SSP of polyamides should follow second-order kinetics. In this case, the overall rate of polymerization can be written as

$$R_p = k_p[\mathrm{M_1}^*][\mathrm{M_2}^*] \tag{25}$$

The jump distance, or critical reaction distance, is obtained from eqs 24 and 25 as

$$\delta = \left[\frac{3k_p}{2\pi N_a\rho_A k_i[\mathrm{A}^*]}\right]^{1/3} \tag{26}$$

It should be noted that eq 26 is valid whether a stoichiometric balance is present in the system.

Validation of the Governing Mechanism and Kinetic Model. To validate the proposed mechanism for end-group migration in solid-state polymerization, experimental molecular weight data were used to calculate the hop distance associated with interchange and polymerization reactions in the solid-state polym-

Table 3. Amine–amide Interchange Reaction Rate Constants for Nylon 66 as Estimated from the Kinetic Model, Obtained Assuming a Noncrystalline Density of 1 G/cm^3

temperature °C	rate constant (mol/g)$^{-1}$ s^{-1}
220	0.53
230	1.27
240	2.00
250	7.07

erization of nylon 66. This was also used to obtain the activation energy for amine–amide interchange, which we compared to the value published in the literature.

With stoichiometric balance in nylon 66, the concentration of end groups in the noncrystalline phase is

$$[\mathrm{M}^*] = [\mathrm{M}_1^*] = [\mathrm{M}_2^*] = \frac{[\mathrm{M}]}{(1 - X_c)} \tag{27}$$

Assuming $M_w \approx M_v$ and $M_w/M_n \approx 2$, the rate of polymerization can be calculated, using the second-order rate constant from the experimental data of viscosity-averaged molecular weight versus time, as follows:

$$R_p = k_p \frac{1}{M_n^{\,2}(1 - X_c)^2} = k_p \frac{4}{M_v^{\,2}(1 - X_c)^2} \tag{28}$$

For nylon 66, the calculations were made using the second-order rate constant for solid-state polymerization at 240 °C, and assuming a weight fraction crystallinity, X_c, of 30%, as obtained from X-ray measurements, an overall density of 1.14 g/cm^3 (as measured by Helium pycnometry), an amorphous density of 1 g/cm^3,[23] and an initial number average molecular weight of 20 000 g/mol (as obtained from experimental data,[3] assuming a polydispersity index of 2). By using an interchange reaction rate constant of 2 cm^3 of noncrystalline phase mole^{-1} s^{-1} at 240 °C,[23] and assuming a noncrystalline density of 1 g/cm^3 at this temperature, the diffusion jump distance is found to be 5.12 Å. This estimate is in excellent agreement with the 5–6 Å which has been obtained as the critical reaction distance from classical studies of diffusion-controlled reactions of small molecules.[19,24] The corresponding overall rate of polymerization is 1.84×10^{-8} mol (g of noncrystalline phase)$^{-1}$ s^{-1} and an interchange reaction frequency of 0.0177 s^{-1} per end group at 240 °C. The effective "chemical" diffusion coefficient for amine functionality is then found to be 5.122×10^{-18} cm^2/s per end group.

As a further check, interchange rate constants for nylon 66 were calculated using the calculated rate of polymerization from the experimentally observed data at 220, 230, and 250 °C, and the critical reaction distance (hop distance) was calculated at 240 °C using the current kinetic model. It is assumed that the critical reaction distance does not change with temperature. The calculated rate constants for interchange are given in Table 3. With the critical reaction distance assumed to be independent of temperature, the activation energy for interchange reaction is the same as the activation energy for the overall rate of polymerization. Thus, the activation energy for interchange reaction is found to be 42 kcal/mol, in the range of known activation energies of interchange reactions in polyamides.[10] Also, it should be noted that this activation energy is 4–8 times the activation energies for physical diffusion, which will be obtained if the SSP process is controlled by physical diffusion of chain segments which carry the functional groups for polymerization. These inferences from the diffusion model and the experimental data corroborate well the premise that interchange reactions provide the dominant mechanism for functional group migration in solid-state polymerization.

Solid-State Polymerization of Polyesters. Solid-state polymerization was also carried out in melt-spun filaments of poly(ethylene terephthalate). Intrinsic viscosities in excess of 2.4 dL/g (solvent hexafluoro-2-propanol) after 2 h of SSP at 240 °C were reported for solid-state polymerized samples which were sent to an industrial analytical laboratory for analysis. Thus, molecular weights up to at least 117 000 g/mol were obtained from a starting molecular weight of 30 000 g/mol.[17] GC/MS analysis of the byproduct from solid-state polymerization confirmed that linear chain extension occurred. More importantly, it was found that, by choosing the precursors with appropriate morphological characteristics, the ductility of the fibers could be retained after SSP, facilitating further drawing. However, getting accurate kinetic data for polyesters, especially those corresponding to long SSP times, is made difficult by the poor solubility of the high molecular weight products.

The kinetic scheme presented for polyamides can also be used to model solid-state polymerization of polyesters. In this case, the two reactions which can cause migration of end-group functionality are the alcohol–ester interchange and the acid–ester interchange reactions. The rate of the acid–ester interchange reaction is known to be much slower than that of the alcohol–ester interchange reaction.[1] Also, bulk polymerization of commercial polyesters is carried out through ester interchange in the polycondensation step. For example, PET is usually produced from diethylene glycol terephthalate, formed through either direct esterification of terephthalic acid or exchange reaction of dimethyl terephthalate with excess ethylene glycol. In this case, since the polymerization reaction is also the alcohol–ester interchange reaction, the critical distance for polymerization reaction, δ_E , is the same as the critical distance for interchange reaction for functional group migration. The generalized reaction rate for the alcohol–ester interchange reaction, R_3, can be written as

$$R_3 = k_3[\mathrm{M}_3^*]^m[\mathrm{E}^*]^n \tag{29}$$

where k_3 is the rate constant for the alcohol–ester interchange reaction, [M$_3$*] is concentration of alcohol end group in the noncrystalline phase, and [E*] is the ester group concentration in the noncrystalline phase. Since the reactions with the ester groups at the end of molecules constitute the polymerization reactions, the rate of migration of functionality is given by the total rate of alcohol–ester interchange, minus the rate of polymerization reactions, i.e.,

$$R_m = k_3[\mathrm{M}_3^*]^m([\mathrm{E}^*]^n - [\mathrm{M}_4^*]^n) \tag{30}$$

where [M$_4$*] is the concentration of ends in the noncrystalline phase. (Note: [M$_3$*] = [M$_4$*].) Therefore, proceeding as for polyamides, the effective diffusion coefficient for alcohol end group functionality, D_3, is found to be

$$D_3 = {}^1/_6\,\delta_E^{\,2} k_3[\mathrm{M}_3^*]^{m-1}([\mathrm{E}^*]^n - [\mathrm{M}_3^*]^n) \tag{31}$$

Table 4. Possible Reactions and Their Morphological Consequences during Solid-State Polymerization

	amide in loop	amide in bridge	amide in AC	amide in FC	amine in AC	amine in FC
amide in loop	no change or B+B	no change	L+AC or B+AC	AC + AC	B+AC or no change	AC+AC
amide in bridge		B+B or L+L	B+AC or L+AC	AC + AC	L+AC or no change	AC+AC
amide in AC			no change or L+FC or B+FC	no change	L+FC or B+FC	no change
amine in AC					TL, BL or BC	AC
amine in FC						FC

An equation similar to eq 23 can be obtained for the polymerization rate,on the basis of on the rate of encounters. By using eq 31, the rate of transesterification-based polymerization in polyesters is then found to be

$$R_p = {}^2/_3\pi\delta_E{}^3 k_3([E^*]^n - [M_3^*]^n)[M_3^*]^m[M_3^*]N_a \quad (32)$$

At the high molecular weights, such as those in postextrusion solid-state polymerization, the concentration of ends is negligible compared to the ester concentration. Since ester interchange is a first-order reaction in $[M_3^*]$ and $[E^*]$, eq 32 can then be written as

$$R_p \cong {}^2/_3\pi\delta_E{}^3 k_3[E^*][M_3^*]^2 N_a\rho_A \quad (32)$$

In this case, the overall rate of polymerization also can be written as

$$R_p = k_p[M_3^*]^2 \quad (33)$$

where the effective rate constant, k_p, is found to be

$$k_p = {}^2/_3\pi\delta_E{}^3 k_3[E^*]N_a\rho_A \quad (34)$$

Thus, the overall rate constant can provide a measure of the critical reaction distance, and vice-versa. However, to verify the kinetic scheme for the solid-state polymerization of polyesters, accurate polymerization data are required.

Morphological Implications. Interchange reactions can have profound implications with regard to the morphology of semicrystalline polymers, since they have the potential to produce a structural reorganization with respect to the relative concentrations of the different topological components of the noncrystalline phase. These topological components are single anchor chains, loops (or folds), bridging chains (or tie chains), and free chains. The existence of loops (folds) and bridges (tie chains) in a semicrystalline material especially affects the mechanical properties of the material.

This field of investigation has been largely neglected, although "it offers new prospects in polymer physics and chemistry".[1] Interchange reactions can result in the formation or elimination of intercrystalline loops and bridges. It has to be noted that one reaction can have several issues, and thus several morphological consequences. For example, as shown in Figure 5, an anchor chain can react with a bridging chain to form a loop, or a (substitute) bridging chain, and another anchor chain.

As a first step toward understanding the potential morphological consequences of interchange reactions during postextrusion SSP, a simplified kinetics-based morphological model was formulated to demonstrate the possible evolution in concentrations of the four types of topological segments. This is exemplified through an analysis of nylon 66. All end groups are considered to be in the noncrystalline phase and all reactions are considered to occur in this phase. If N represents the average number of amide groups in the different kind

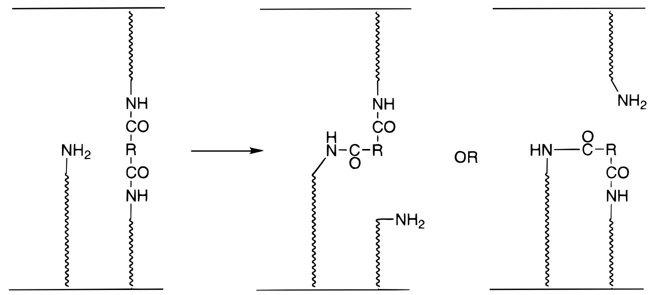

Figure 5. Example of the morphological effects of amine−amide interchange reaction in intercrystalline domains of polyamides.

of topological segments (anchor chains, loops, bridges, and free chains), the amide concentration in the noncrystalline phase C^* can be related to the concentrations of chains as follows:

$$C^* = N_{AC}C_{AC} + N_LC_L + N_BC_B + N_{FC}C_{FC} \quad (35)$$

where N_{AC}, N_L, N_B, and N_{FC} are the number of anchor chains, loops, bridges, and free chains respectively, and C_{AC}, C_L, C_B, and C_{FC} their corresponding concentrations.

The possible different reactions (polymerization and interchange) are listed in Table 4. Considering all possible reactions, the change in concentration of any topological segment can be obtained from the equations governing the rates of the different reactions. The evolution of concentration of topological segments with time can be described mathematically as follows:

$$dC_{AC}/dt = -{}^1/_2k_pC_{AC}{}^2 - kNC_{AC}{}^2 + 4kNC_{AC}C_L + 4kNC_{FC}C_B \quad (36)$$

$$dC_L/dt = {}^1/_2k_pC_{AC}{}^2 + kNC_{AC}{}^2 - 4kNC_{AC}C_L + {}^1/_24kNC_{AC}C_B - 2kNC_{FC}C_L \quad (37)$$

$$dC_B/dt = -{}^1/_8k_pC_{AC}{}^2 + {}^1/_4kNC_{AC}{}^2 + {}^1/_2kNC_{AC}C_L - {}^1/_2\, kNC_{AC}C_B - 2kNC_{FC}C_B \quad (38)$$

$$dC_{FC}/dt = -k_pC_{FC}{}^2 - k_pC_{AC}C_{FC} + {}^1/_2kNC_{AC}{}^2 - 2kNC_{FC}C_L - 2kNC_{FC}C_B \quad (39)$$

where k_p is the rate constant for polymerization and k, the rate constant of amine−amide interchange reaction. The amide−amide interchange reaction was neglected but it could be included in the above equations, if necessary.[17] In this simplified model, loops, and bridges are considered to be twice as long, each with an average of $2N$ monomer units, as anchor and free chains, each with an average of N monomer units. Also, preferences in reactions which might be dictated by differences in the free energies of topologically different chains are ignored. In addition, the calculations were performed assuming the concentration of free chains to be negligible. The system of differential equations, eqs 36−39, was solved using the polymerization and interchange rate constants for nylon 66 given earlier, beginning with an initial number average molecular weight of 20 000 g/mol. The calculations were performed for an average number of ten monomer units per topological segment. Figure 6 presents the evolution of loop fraction, R_L, and the bridge fraction, R_B, calculated from

$$R_L = \frac{C_L}{C_L + C_B} \tag{40}$$

$$R_B = \frac{C_B}{C_L + C_B} \tag{41}$$

for two different cases: a starting material with only loops and a starting material with only bridges. For the two starting morphologies, the concentrations of loops and bridges reach a steady-state concentration after a certain time of polymerization, with the number of loops equal to the number of bridging chains. This last outcome comes from the assumption of no influence of the topology or the length of a chain on the reaction rate. *Thermodynamic preferences for the formation of different topological segments, dictated by intrinsic rigidity of the polymer, would affect the final loop-to-bridges ratio.* A more rigorous formulation to account for this aspect is currently being carried out.

The kinetics-based morphological model serves to demonstrate how the underlying mechanism of solid-state polymerization can produce significant changes in the concentrations of topologically different chains in intercrystalline domains. However, the gross oversimplifications here preclude valid *quantitative* predictions of the evolution of morphology during SSP. The probabilities of reactions with different topological consequences, such as loops and bridges, as well as the chain length distribution of the different types of topological segments have to be taken into account. It should be apparent that the intrinsic rigidity of a molecular segment and its length would dictate its preferential existence as a loop or a bridge in an intercrystalline region. To predict the differences in the evolution of morphology which can occur during postextrusion solid-state polymerization of different polymers, we are currently developing a thermodynamic framework to address these issues.

Concluding Remarks

The research reported here addresses the comprehensive interactive aspects of the mechanisms, kinetics, and potential morphological consequences of postextrusion SSP of polyesters and polyamides. It has yielded the following important conclusions.

• When SSP of the condensation type is carried out on extruded geometries which offer a short distance for diffusional escape in at least one direction, the process is no longer limited by the rate/probability of removal of the condensation molecule, i.e., any kinetic limitation due to the reverse reaction becomes negligible. This facilitates a substantial increase in molecular weight in a single stage process. For example, up to a 7-fold increase in molecular weight in nylon 66, a 4-fold increase in poly(ethylene terephthalate), and a 3-fold increase in nylon 46 have been achieved. Such geometries also allow exploration of the fundamental mechanisms governing migration and "reactive collision" of functional groups, without the complications which can arise from a high probability of the reverse (depolymerization) reaction of the condensation product before its release from the material.

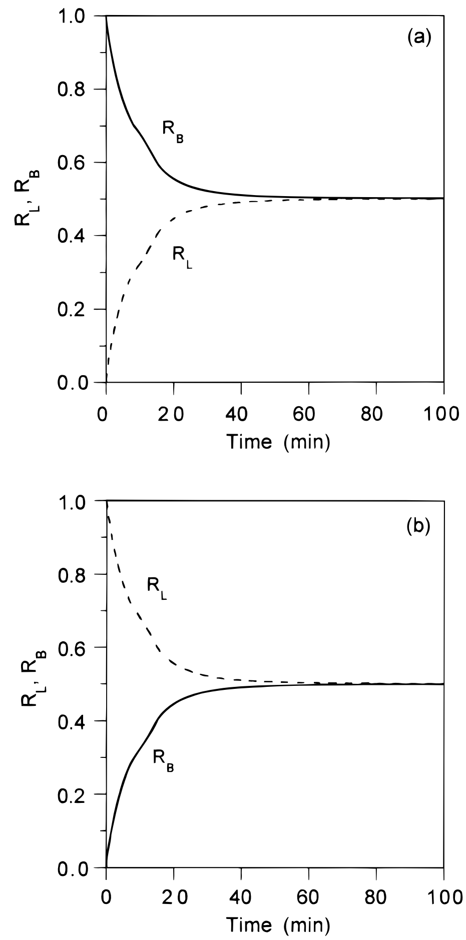

Figure 6. Loop (R_L) and bridge (R_B) fraction as a function of polymerization time. These predictions are from a simplified model that neglects any thermodynamic preferences for topologically different chains or for chains of different lengths (see text for details): (a) starting materials with only bridges and (b) starting material with only loops. Lines: solid, bridge fraction; dotted, loop faction.

• "Migration of functionality" via interchange reactions, not molecular or segmental diffusion, is the facilitating or limiting mechanism which allows two functional groups to approach each other within the required distance for "chain extension".

• Kinetics of migration of functionality via interchange, chemical diffusion, and polymerization has exactly the same mathematical form as that of classical statistical mechanics of (physical) diffusion-controlled reactions of small molecules. The consequent overall rate of solid-state polymerization in both polyamides and polyesters corresponds to simple step growth kinetics. The estimate obtained for the critical amine−amide interchange reaction distance from this formulation, 5.1 Å, is in excellent agreement with the 5−6 Å reported from classical studies of diffusion-controlled reactions.

• The mechanism which governs migration of functionality in SSP can have a profound implication with regard to the formation or the elimination of loops and intercrystalline bridges of flexible and semirigid segments, as well as strained and unstrained intercrystalline bridges of rigid segments, in oriented polymer morphologies. The potential implications of this mechanism vis-à-vis formation of high-performance morphologies in fibers and films of semirigid polymers are being explored.

Acknowledgment. The authors gratefully acknowledge partial funding of this research through a grant from the DuPont Company to Georgia Tech's Polymer Program Associates. One of the authors, Celine Almonacil, was also partially funded by the Molecular Design Institute.

References and Notes

(1) Schultz, J. M.; Fakirov, S. In *Solid State Behavior of Linear Polyesters and Polyamides*; Prentice Hall: Englewood Cliffs, NJ, 1990; p 11 and 19.
(2) Pilati, R. In *Comprehensive Polymer Science*; Pergamon: New York, 1989; Vol. 5, p 201.
(3) Srinivasan, R.; Desai, P.; Abhiraman, A. S.; Knorr, R. S. *J. Appl. Polym. Sci.* **1994**, *53*, 1731.
(4) Chen, F. G.; Griskey, R. G.; Beyer, G. H. *AIChE J.* **1969**, *15*, 680.
(5) Gaymans, R. J.; Amirtharaj, J.; Kamp, H. *J. Appl. Polym. Sci.* **1982**, *27*, 2513.
(6) Mallon, F. K.; Ray, W. H. *J. Appl. Polym. Sci.* **1998**, *69*, 1233.
(7) Mallon, F. K.; Ray, W. H. *J. Appl. Polym. Sci.*, to appear.
(8) Kaushik, A.; Gupta, S. K. *J. Appl. Polym. Sci.* **1992**, *45*, 507.
(9) Chen, S.; Chen, F. L. *J. Polym. Sci., Polym. Chem. Ed.* **1987**, *25*, 533.
(10) Kotliar, A. M. *J. Polym. Sci.* **1981**, *16*, 367.
(11) Droscher, M.; Schmidt, F. G. *Polym. Bull.* **1981**, *4*, 261.
(12) McAlea, K. Ph.D. Thesis, University of Delaware, 1984.
(13) Lenz, R. W.; Schuler, A. N. *J. Polym. Sci., Polym. Symp.* **1978**, *63*, 343.
(14) Lenz, R. W.; Jin, J.-I.; Feichtinger, K. A. *Polymer* **1984**, *24*, 327.
(15) Fitzgerald, J. A.; Irwin, R. S.; Memeger, W. *Macromolecules* **1991**, *24*, 11.
(16) Since no values could be found in the literature, these were calculated using the QSPR module of the Insight II molecular modeling software.
(17) Srinivasan, R. Ph.D. Thesis, Georgia Institute of Technology, 1994.
(18) Roerdink, K.; Warnier, J. M. M. *Polymer* **1985**, *26*, 1582.
(19) Hammes, G. G. In *Principles of Chemical Kinetics*; Academic Press: New York, 1978; Vol. 62, pp 62−65.
(20) Chandrasekhar, S. *Rev. Mod. Phys.* **1943**, *15*, 1.
(21) McQuarrie, D. A. In *Statistical Mechanics*; Harper and Row: New York, 1976; p. 514.
(22) Private communication from industry sources.
(23) Estimate of the amorphous density at $T = 240$ °C. Room-temperature amorphous density is reported to be 1.07 g/cm^3. (Van Krevelen, D. W. In *Properties of Polymers, Their Estimation and Correlation with Chemical Structure*; Elsevier Scientific: Amsterdam, 1976.)
(24) Barrow, G. M. In *Physical Chemistry*; McGraw-Hill Kogakusha: Tokyo, 1979; pp 690−693.

MA980693S